Effect of secondary electron emission on nonlinear dust acoustic wave propagation in a complex plasma with positive equilibrium dust charge

Subrata Bhakta and , and Susmita Sarkar

Citation: Physics of Plasmas **24**, 073706 (2017); doi: 10.1063/1.4990553
View online: http://dx.doi.org/10.1063/1.4990553
View Table of Contents: http://aip.scitation.org/toc/php/24/7
Published by the American Institute of Physics

Effect of secondary electron emission on nonlinear dust acoustic wave propagation in a complex plasma with positive equilibrium dust charge

Subrata Bhakta[1,a)] and Susmita Sarkar[2,b)]
[1]Department of Mathematics, S.A. Jaipuria College, Kolkata, India
[2]Department of Applied Mathematics, University of Calcutta, Kolkata, India

(Received 23 February 2017; accepted 13 June 2017; published online 11 July 2017)

In this paper, we have investigated the effect of secondary electron emission on nonlinear propagation of dust acoustic waves in a complex plasma considering equilibrium dust charge positive and compared the results with those obtained in our recently published paper [Bhakta *et al.*, Phys. Plasmas **24**, 023704 (2017)] where the equilibrium dust charge was negative. In both papers, primary and secondary electrons are assumed to follow Boltzmann distribution with separate electron temperatures, ions are also Boltzmann distributed, and charged dust grains are inertial. Change in the nature of dust charge (negative to positive) gives rise to some opposite behaviour of wave propagation characteristics in dusty plasma when dust grains are charged by secondary electron emission mechanism. Both adiabatic and nonadiabatic dust charge variations have been separately considered in both the papers. The investigation in this paper shows that compressive dust acoustic soliton propagates in case of adiabatic dust charge variation whose amplitude increases and width decreases with an increase in the strength of the secondary electron emission. This is in contrast to the case of negative equilibrium dust charge which confirms the existence of rarefied dust acoustic soliton with decreasing amplitude and increasing width for an increase in the strength of the secondary electron emission. Nonadiabaticity of dust charge variation in both cases generates dust acoustic shock wave which is oscillatory for weak nonadiabaticity and monotonic for strong nonadiabaticity. For positive equilibrium dust charge, the amplitude of both oscillatory and monotonic shocks increases and oscillation of the oscillatory shock persists longer for stronger secondary electron emission. On the other hand for negative equilibrium dust charge, the amplitude of both the oscillatory and monotonic shocks diminishes with increasing secondary electron emission. *Published by AIP Publishing.*
[http://dx.doi.org/10.1063/1.4990553]

I. INTRODUCTION

Charging of dust grains by secondary electron emission (SEE) is an important grain charging process in space and astrophysical plasmas. When an energetic electron hits a dust grain and enters the material, it excites secondary electrons which ultimately leaves the material.[1] This effect has been studied in material science,[2] astrophysics,[3–5] and space plasmas.[6,7] Such energetic electrons are also present in earth's atmosphere which generate different auroral phenomena.[8] Secondary electron emission has also an effect on the charge state of satellites when they orbit low over the poles within the auroral regions.[9]

Secondary electron current produced by emitted electrons flows out of the dust grains. This may cause either negative or positive grain charging accordingly as the magnitude of the secondary electron yield (ratio of the emitted electrons to the incident electrons) is low or high. This magnitude depends on the energy of the incident electrons and the nature of the dust material.[10–16]

Observations made during Apollo missions indicated that the Moon's surface and lunar dust grains are electrostatically charged, positively during the lunar day and negatively during the lunar night. Observations confirmed that submicron sized positively charged particles at low surface potentials generally charge more positively when exposed to low energy electrons (<25 eV) and discharge at higher energies (>100 eV). Thus, the secondary electron emission yields are higher for smaller particles than the larger.[27] On the other hand, dust grains will be charged positively independent of the grain size in case of solar light illumination because of the low plasma temperature. For large plasma temperature, smaller grains achieve very high potential.[34] In this paper, we shall consider only positive equilibrium dust charge, i.e., higher secondary electron emission to study the effect of secondary electron emission on nonlinear dust acoustic wave propagation in a complex plasma. Similar study has been recently reported considering the negative equilibrium dust charge.[28] Main objective of this paper is to compare the results obtained in these two cases.

Secondary electron emission from dust grains influences wave propagation characteristics in dusty plasmas. Gupta *et al.*[17,18] first studied the linear theory of low frequency dust acoustic and dust ion acoustic wave propagation in the presence of secondary electron emission in complex plasma.[19] The presence of nonthermal electrons has also been considered to study its linear theory.[20] Later, this secondary electron emission effect on the growth rate of Jeans instability was investigated in the presence of both thermal and nonthermal ions.[21–23] Nonlinear theory of dust acoustic

a)E-mail: subratabhakta88@gmail.com
b)E-mail: susmita62@yahoo.co.in

wave propagation in the presence of secondary electron emission has been recently reported considering the negative equilibrium dust charge and both adiabatic and nonadiabatic dust charge variations.[28]

Adiabatic dust charge variation is a fast grain charging process whose effect on nonlinear dust acoustic wave propagation has been studied by several authors in both unmagnetized and magnetized dusty plasmas.[29–33] But none of them considered the effect of secondary electron emission. Our present analysis shows that in the presence of positively charged dust grains with adiabatic dust charge variation, secondary electron emission generates compressive dust acoustic soliton whose amplitude increases and width decreases with an increase in the strength of secondary electron emission. Thus for strong secondary electron emission, dust acoustic soliton moves faster when equilibrium dust charge is positive. This is in contrary to the case when equilibrium dust charge is negative as in the presence of negatively charged dust grains, rarefied dust acoustic soliton propagates whose amplitude decreases, width increases, and consequently velocity decreases with increasing secondary electron emission.[28]

On the other hand, nonadiabatic dust charge variation is a slow grain charging process. It induces Burger like dissipative effect which gives rise to dust acoustic shock wave. This compresses dust density across the shock and hence may be a mechanism of star formation. Star birth always takes place in dusty environment. Nonadiabatic dust charge variation thus plays an important role in the star forming regions of the universe, e.g., inside the orion nebula in the milky way or in the tarantula, the brightest star forming region of the universe.[37–39]

The theory of the nonadiabatic dust charge variation was first developed by Gupta *et al.*[24] which was applied to study the nonlinear evolution of small amplitude low frequency waves in dusty plasmas.[25,26,31,35] Recently, Wang *et al.*[36] studied this effect in strongly coupled dusty plasmas. But in none of those studies, effect of secondary electron emission was considered. Secondary electron emission effect in the study of nonlinear dust acoustic wave propagation in the presence of nonadiabatic dust charge variation has been first time reported by us considering equilibrium dust charge negative.[28] Since two stable equilibrium dust charge states exist in a dusty plasma when dust grains are charged by secondary electron emission mechanism, out of which one is negative and the other is positive, we have considered in this paper the presence of positive equilibrium dust charge to study the same phenomena reported in Ref. 28 for equilibrium dust charge negative. Both results have been compared in the present paper.

Our results in this paper show that in the presence of positively charged dust grains, nonadiabaticity of dust charge variation induces dust acoustic shock wave which is dispersion dominated and hence oscillatory for weak nonadiabaticity and dissipation dominated and hence monotonic for strong nonadiabaticity. For both weak and strong nonadiabaticities, the dissipation (nonadiabaticity induced) coefficient and hence the dissipation–dispersion ratio decrease at stronger secondary electron emission. Hence, higher secondary electron emission helps to lose monotonicity and gain dispersive character of the dust acoustic shock wave. In addition, the amplitude of both oscillatory and monotonic shocks in this case increases with increasing secondary electron emission. This is just the opposite situation for the case when equilibrium dust charge is negative where higher secondary electron emission diminishes the amplitude of both oscillatory and monotonic shocks and increases the monotonicity of the dust acoustic shock wave.

Stability analysis of the KdV-Burger equation in this paper shows that the equilibrium point with zero potential is a saddle and hence is unstable whereas the equilibrium point with nonzero potential is a stable node or stable focus, provided a cut off condition is satisfied. This cut off reduces with increasing secondary electron emission which enhances the chance of the nonzero equilibrium point being a stable focus that pronounces the oscillatory character of the dust acoustic shock wave. This is just opposite to Ref. 28.

Positively charged dust grains generated by secondary electron emission exist in solar wind environment whose surface potential is independent of the grain size. Our proposed model may be applicable in this case as we have not considered grain size variation.

II. BASIC EQUATIONS

The dust acoustic wave is a very low frequency wave whose thermal velocity is very small compared to both electron and ion thermal velocities. So, it does not respond to both electrons and ions, and hence, electron and ion inertia can be neglected in its study. Only dust inertia in this case is important. Hence, plasma under our consideration consists of Boltzmann distributed primary and secondary electrons, ions, and positively charged inertial dust grains. Primary and secondary electron temperatures are assumed unequal. These four components satisfy the quasineutrality condition

$$n_{io} + z_{d0} n_{d0} = n_{eo} + n_{so}, \tag{1}$$

where n_{io}, n_{eo}, n_{so}, and n_{d0} are equilibrium number densities of ions, primary electrons, secondary electrons, and dust grains, respectively, and z_{d0} is the number of charges on dust grains in equilibrium. This quasi-neutrality condition differs from the quasi-neutrality condition for negative equilibrium dust charge.[28] For positive equilibrium dust charge, the density ratio $\frac{n_{i0}}{n_{e0}}$ is less than $(1+\frac{n_{s0}}{n_{e0}})$, whereas for negative equilibrium dust charge, it is greater than one.

The normalized basic equations satisfied by the Boltzmann distributed primary electrons, secondary electrons, ions, and inertial charged dust grains are

$$\mathrm{N_e} = \exp(\Phi), \tag{2}$$

$$\mathrm{N_i} = \exp\left(-\frac{\Phi}{\sigma_\mathrm{i}}\right), \tag{3}$$

$$\mathrm{N_s} = \exp\left(\frac{\Phi}{\sigma_\mathrm{s}}\right), \tag{4}$$

$$\frac{\partial \mathrm{N_d}}{\partial \mathrm{T}} + \frac{\partial}{\partial \mathrm{X}}(\mathrm{N_d V_d}) = 0, \tag{5}$$

$$\frac{\partial \mathrm{V_d}}{\partial \mathrm{T}} + \mathrm{V_d}\frac{\partial \mathrm{V_d}}{\partial \mathrm{X}} = -\frac{\mathrm{Q_d}}{\alpha_\mathrm{d}}\frac{\partial \Phi}{\partial \mathrm{X}}, \tag{6}$$

$$\left(\frac{\omega_{pd}}{\nu_d}\right)\left(\frac{\partial Q_d}{\partial T}+V_d\frac{\partial Q_d}{\partial X}\right)=\frac{1}{\nu_d}\left(\frac{\bar{I}_i+\bar{I}_e+\bar{I}_e^s}{z_{do}e}\right), \tag{7}$$

$$\frac{\partial^2\Phi}{\partial X^2}=-\frac{1}{\left(1+\frac{\delta_i}{\sigma_i}+\frac{\delta_s}{\sigma_s}\right)}\left(\delta_i\exp\left(-\frac{\Phi}{\sigma_i}\right)-\exp(\Phi)-\delta_s\exp\left(\frac{\Phi}{\sigma_s}\right)+(1-\delta_i+\delta_s)Q_dN_d\right). \tag{8}$$

Here, the primary electron, secondary electron, ion, and dust number densities n_e, n_s, n_i, n_d, dust fluid velocity u_d, electrostatic potential energy $e\phi$, dust charge q_d, and the independent space, time variables x, t are normalized in the following way:

$$X=x/\lambda_d;\quad T=\omega_{pd}t;\quad N_d=n_d/n_{d0};\quad N_i=n_i/n_{i0};$$
$$N_e=n_e/n_{e0};\quad N_s=n_s/n_{s0};\quad V_d=u_d/c_d;$$
$$\Phi=\frac{e\phi}{T_e};\quad Q_d=q_d/ez_{d0},\quad q_{do}=z_{do}e, \tag{9}$$

where $\lambda_D=\left(\frac{T_{eff}}{4\pi z_{d0}n_{d0}e^2}\right)^{1/2}$ is the dusty plasma Debye length and $c_d=\sqrt{\frac{z_{d0}T_{eff}}{m_d}}$ is the dust acoustic speed, implying $c_d^2=\lambda_D^2\omega_{pd}^2$. The effective temperature T_{eff} is defined by the relation

$$\frac{1}{T_{eff}}=\frac{1}{z_{do}n_{do}}\left(\frac{n_{io}}{T_i}+\frac{n_{eo}}{T_e}+\frac{n_{so}}{T_s}\right). \tag{10}$$

Here, T_e, T_s, and T_i are primary electron, secondary electron, and ion temperatures, respectively, and $\sigma_i=\frac{T_i}{T_e}$, $\sigma_s=\frac{T_s}{T_e}$, $\delta_i=\frac{n_{io}}{n_{eo}}$, $\delta_s=\frac{n_{so}}{n_{eo}}$, $\alpha_d=\frac{(1-\delta_i+\delta_s)}{(1+\frac{\delta_i}{\sigma_i}+\frac{\delta_s}{\sigma_s})}$, $z=z_{d0}e^2/r_0T_e$, q_{do} is the equilibrium dust charge, and r_0 is the grain radius.

The nondimensionalized expressions $\bar{I}_i$ and $\bar{I}_e$ for ion and primary electron current flowing to the dust grains and $\bar{I}_e^s$ for the secondary electron current flowing out of the dust grains are

$$\bar{I}_i=\pi r_0^2e\sqrt{\frac{8T_i}{\pi m_i}}n_{i0}\exp\left(-\frac{\Phi}{\sigma_i}\right)\exp\left(-\frac{zQ_d}{\sigma_i}\right), \tag{11}$$

$$\bar{I}_e=-\pi r_0^2e\sqrt{\frac{8T_e}{\pi m_e}}n_{e0}\exp(\Phi)(1+zQ_d), \tag{12}$$

$$\bar{I}_e^s=3.7\delta_M\pi r_0^2e\sqrt{\frac{8T_e}{\pi m_e}}n_{e0}\exp(\Phi)\left(1+\frac{zQ_d}{\sigma_s}\right)\times\exp\left(zQ_d-\frac{zQ_d}{\sigma_s}\right)F_{5,B}\left(\frac{E_M}{4T_e}\right), \tag{13}$$

where m_i, m_e are ion and electron masses and δ_M is the maximum yield of secondary electrons which occurs when the impinging electrons have the maximum kinetic energy E_M. The function $F_{5,B}(x)$ is given by[10]

$$F_{5,B}(x)=x^2\int_B^\infty u^5\exp[-(xu^2+u)]du,\quad\text{where}$$
$$x=\frac{E_M}{4T_e}\quad\text{and}\quad B=\sqrt{\frac{\frac{eq_d}{r_0T_e}}{x}}. \tag{14}$$

The expressions for $\bar{I}_i$, $\bar{I}_e$ and $\bar{I}_e^s$ in (11), (12), and (13) here are different from their expressions for negative equilibrium dust charge.[28] The differences in the quasi neutrality condition (1) and the current expressions (11)–(13) are the origin of the difference in the behaviour of wave propagation characteristics for the two cases of equilibrium dust charge negative and positive.

The grain charging frequency in this case has been calculated in the form,

$$\nu_d=-\frac{\partial(\bar{I}_i+\bar{I}_e+\bar{I}_e^s)}{\partial Q_d}\Big|_{Q_d=z_de}=\frac{a}{\sqrt{2\pi}}\frac{\omega_{pi}^2}{V_{thi}}\left[\exp\left(-\frac{z}{\sigma_i}\right)+\frac{\alpha_{2s}\sqrt{\mu_i\sigma_i}}{\delta_i}\right], \tag{15}$$

where

$$\alpha_{2s}=1-3.7\delta_M\exp\left(z-\frac{z}{\sigma_s}\right)\times\left\{\frac{1}{\sigma_s}+\left(1+\frac{z}{\sigma_s}\right)\left(1-\frac{1}{\sigma_s}\right)\right\}F_{5,B_0}\left(\frac{E_M}{4T_e}\right). \tag{15a}$$

The grain charge number z is not arbitrary. It satisfies the condition δ_i $(=\frac{n_{io}}{n_{eo}})$ less than $(1+\delta_s)$ as the equilibrium dust charge is positive. The equilibrium current balance equation in this case gives[28]

$$\delta_i=\sqrt{\mu_i}\frac{(1+z)\alpha_{1s}}{\sqrt{\sigma_i}}\exp\left(\frac{z}{\sigma_i}\right)\text{as a function of } z(=z_{d0}e^2/r_0T_e), \tag{16}$$

with $\alpha_{1s}=1-3.7\delta_M\exp(z-\frac{z}{\sigma_s})F_{5,B_0}\left(\frac{E_M}{4T_e}\right)(1+\frac{z}{\sigma_s})/(1+z)$, and $\mu_i=\frac{m_i}{m_e}$.

Thus, z must be determined from the inequality

$$\sqrt{\frac{m_i}{m_e}}\frac{(1+z)\alpha_{1s}}{\sqrt{\sigma_i}}\exp\left(\frac{z}{\sigma_i}\right)<1+\delta_s. \tag{17}$$

III. REDUCTIVE PERTURBATION ANALYSIS: ADIABATIC AND NONADIABATIC DUST CHARGE VARIATION

Now for the study of small amplitude structures in dusty plasma in the presence of secondary electron emission with positive equilibrium dust charge, we employ the reductive perturbation technique, using the stretched coordinates $\xi=\varepsilon^{1/2}(X-\lambda T)$ and $\tau=\varepsilon^{3/2}T$ where ε is a small parameter and λ is the wave velocity normalized by c_d. The variables N_d, V_d, Φ, and Q_d are then expanded as

$$N_d=1+\varepsilon N_{d1}+\varepsilon^2N_{d2}+\cdots$$
$$V_d=\varepsilon V_{d1}+\varepsilon^2V_{d2}+\cdots$$
$$\Phi=\varepsilon\Phi_1+\varepsilon^2\Phi_2+\cdots$$
$$Q_d=1+\varepsilon Q_{d1}+\varepsilon^2Q_{d2}+\varepsilon^3Q_{d3}+\cdots. \tag{18}$$

Here, Q_d has been started from +1 which was started from −1 for negative equilibrium dust charge.[28] Proceeding in the same way as in Ref. 28 with adiabatic dust charge variation (dust charging frequency ν_d is very high compared to dust plasma frequency ω_{pd}, implying $\frac{\omega_{pd}}{\nu_d} \approx 0$), we obtain the K-dV equation

$$\frac{\partial \Phi_1}{\partial \tau} + \mathrm{a}\Phi_1 \frac{\partial \Phi_1}{\partial \xi} + \mathrm{b}\frac{\partial^3 \Phi_1}{\partial \xi^3} = 0, \tag{19}$$

where

$$\mathrm{a} = \mathrm{b}\left[\frac{3}{\lambda^2 \alpha_\mathrm{d}} + 2\alpha_\mathrm{d}\gamma_\mathrm{d} + \gamma_2\right], \quad \mathrm{b} = \frac{\lambda^3}{2} = \frac{1}{2}(1-\alpha_\mathrm{d}\beta_\mathrm{d})^{-3/2}, \tag{20}$$

with

$$\beta_d = \frac{\beta_b}{z\beta_a}, \tag{21}$$

$$\beta_a = \frac{z\delta_i}{\sigma_i^2} - \frac{\delta_i}{\sigma_i} - \sqrt{\frac{\mu_i}{\sigma_i}} + 3.7\delta_M F_{5,B}\sqrt{\frac{\mu_i}{\sigma_i}}\left[\frac{1}{\sigma_s}\exp\left(z - \frac{z}{\sigma_s}\right) + (1+z)\left\{\left(1-\frac{1}{\sigma_s}\right) + z\left(1-\frac{1}{\sigma_s}\right)^2\right\}\right];$$

$$\beta_b = \frac{\delta_i}{\sigma_i} - \frac{z\delta_i}{\sigma_i^2} + \sqrt{\frac{\mu_i}{\sigma_i}}(1+z) - 3.7\delta_M F_{5,B}\sqrt{\frac{\mu_i}{\sigma_i}}\left(1+\frac{z}{\sigma_s}\right) \times \left\{1 + \left(z - \frac{z}{\sigma_s}\right)\right\}$$

and

$$\gamma_d = \frac{\gamma_c}{z\beta_a}, \quad \gamma_c = \gamma_{c1} + \gamma_{c2} + \gamma_{c3}, \tag{22}$$

$$\gamma_{c1} = 0.5\left[\sqrt{\frac{\mu_i}{\sigma_i}}(1+z) - \frac{\delta_i}{\sigma_i^2} - 3.7\delta_M F_{5,B}\sqrt{\frac{\mu_i}{\sigma_i}}\left(1+\frac{z}{\sigma_s}\right)\right];$$

$$\gamma_{c2} = \left[\sqrt{\frac{\mu_i}{\sigma_i}} - \frac{\delta_i}{\sigma_i^2} - 3.7\delta_M F_{5,B}\sqrt{\frac{\mu_i}{\sigma_i}}\left\{\frac{1}{\sigma_s} + \frac{1}{\sigma_s}\left(z - \frac{1}{\sigma_s}\right) + \left(1+\frac{z}{\sigma_s}\right)\left(1-\frac{1}{\sigma_s}\right)\right\}\right](z\beta_d)$$

$$\gamma_{c3} = \left[-\frac{\delta_i}{2\sigma_i^2} - 3.7\delta_M F_{5,B}\sqrt{\frac{\mu_i}{\sigma_i}}\left\{\frac{1}{\sigma_s}\left(1-\frac{1}{\sigma_s}\right) + \left(1-\frac{1}{\sigma_s}\right)^2\left(\frac{1+3z/\sigma_s}{2}\right)\right\}\right](z\beta_d)^2.$$

$\gamma_2 = \left(\frac{\frac{\delta_\mathrm{i}}{\sigma_\mathrm{i}^2} - \frac{\delta_\mathrm{s}}{\sigma_\mathrm{s}^2} - 1)}{(1+\frac{\delta_\mathrm{i}}{\sigma_\mathrm{i}} + \frac{\delta_\mathrm{s}}{\sigma_\mathrm{s}}}\right)$ with normalized phase velocity of the dust acoustic wave $\lambda = \frac{1}{\sqrt{1-\alpha_\mathrm{d}\beta_\mathrm{d}}}$ provided $\alpha_\mathrm{d}\beta_\mathrm{d} \neq 1$. These expressions are different from the corresponding expressions in Ref. 28. Thus, final expressions of the coefficient of nonlinearity a and the coefficient of dispersion b are different in the two cases of equilibrium dust charge positive and negative.

The travelling wave solution of this KdV equation (19) is the bell-shaped soliton

$$\Phi_1 = \Phi_{1\mathrm{m}}\,\mathrm{sech}^2\left[\frac{(\xi - \mathrm{M}\tau)}{\mathrm{w}}\right], \tag{23}$$

with amplitude $\Phi_{1\mathrm{m}} = \frac{3\mathrm{M}}{\mathrm{a}}$ and width $\mathrm{w} = 2\sqrt{\frac{\mathrm{b}}{\mathrm{M}}}$ provided $\alpha_\mathrm{d}\beta_\mathrm{d} \neq 1$. M is the Mach number. Expressions of amplitude and width of the dust acoustic soliton in this case differ from those of Ref. 28 as final expressions of a and b are different in these two cases. Moreover, dependence of the amplitude and width on δ_M through α_{1s} indicates their change with the strength of secondary electron emission which will be shown numerically in Sec. IV of this paper.

In the same way for nonadiabatic dust charge variation where $\frac{\omega_{pd}}{\nu_d}$ is small but finite, assumption of $\frac{\omega_{pd}}{\nu_d} = \nu\sqrt{\varepsilon}$ (where ε is small and ν is of order unity) gives the standard KdV-Burger equation[28]

$$\frac{\partial \Phi_1}{\partial \tau} + \mathrm{a}\Phi_1 \frac{\partial \Phi_1}{\partial \xi} + \mathrm{b}\frac{\partial^3 \Phi_1}{\partial \xi^3} = \mu\frac{\partial^2 \Phi_1}{\partial \xi^2}, \tag{24}$$

with same a and b as in (20) and $\mu = -\frac{\lambda^4 \nu\beta_d}{2\sigma\beta_a}\left[\delta_i \exp\left(-\frac{z}{\sigma_i}\right) + \alpha_{2s}\sqrt{\mu_i\sigma_i}\right]$. The Burger coefficient μ (different from the expression in Ref. 28) is arising exclusively due to nonadiabaticity of grain charge variation.[28] Here, μ is also a function of the secondary electron yield δ_M and hence changes with the change in the strength of the secondary electron emission. Variation of μ with δ_M will be shown in Sec. IV.

Nature of the shock whether monotonic or oscillatory can be determined from the study of local stability of the equilibrium points of the KdV-Burger equation (24). On transforming to the wave frame $\eta = V\tau - \xi$, where V is the wave velocity, this equation reduces to the ordinary differential equation

$$b\frac{d^2\Phi_1}{d\eta^2} + \mu\frac{d\Phi_1}{d\eta} + \left[\frac{\mathrm{a}\Phi_1^2}{2} - V\Phi_1\right] = 0, \tag{25}$$

which has two fixed points $\left(\Phi_1 = 0, \frac{d\Phi_1}{d\eta} = 0\right)$ and $\left(\Phi_1 = \frac{2V}{\mathrm{a}}, \frac{d\Phi_1}{d\eta} = 0\right)$.

The first one $\left(\Phi_1 = 0, \frac{d\Phi_1}{d\eta} = 0\right)$ with zero potential is a saddle point and hence unstable in nature. The second one $\left(\Phi_1 = \frac{2V}{\mathrm{a}}, \frac{d\Phi_1}{d\eta} = 0\right)$ with nonzero potential is a stable node for $\frac{\mu^2}{4b} > V$ and a stable focus for $\frac{\mu^2}{4b} < V$. Since the coefficient of dissipation μ changes with secondary electron yield δ_M, this cut off also changes with change in the strength of secondary electron emission which will be determined numerically.

IV. NUMERICAL ESTIMATION

In our numerical calculation, we have used MgO material for which δ_M takes values 3–25, $\mathrm{E_M}$(eV) $\approx$ 400–1500, $\kappa T_e \approx 2$ eV, $\kappa T_s \approx 3$ eV.[10] Since δ_M is the ratio of the emitted electrons to the incident electrons, for positively charged dust grains δ_M has higher values. We have taken its two values 22 and 24. Also $\delta_s\left(=\frac{n_{s0}}{n_{e0}}\right) = 0.8$ and $\mathrm{M} = 1.2$ have been considered. Figure 1 has been plotted for $\delta_i\left(=\frac{n_{i0}}{n_{e0}}\right)$ versus z to fix the range of z satisfying the quasineutrality condition (1). This range is 0.1 to 0.25. Rest of the figures have been plotted within this range of z. Figures 2 and 3 have been plotted for the amplitude and width of the dust acoustic soliton against normalized grain charge number z at

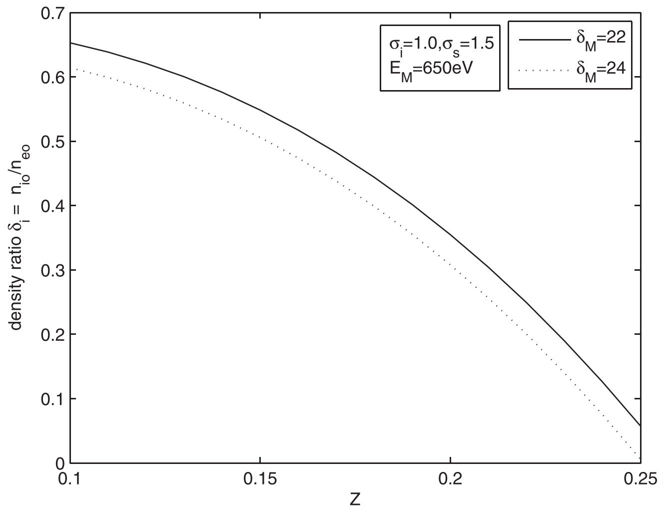

FIG. 1. Plot of $\delta_i(=\frac{n_{i0}}{n_{e0}})$ versus $z\left(=\frac{z_{do}e^2}{r_0 T_e}\right)$ for equilibrium dust charge negative.

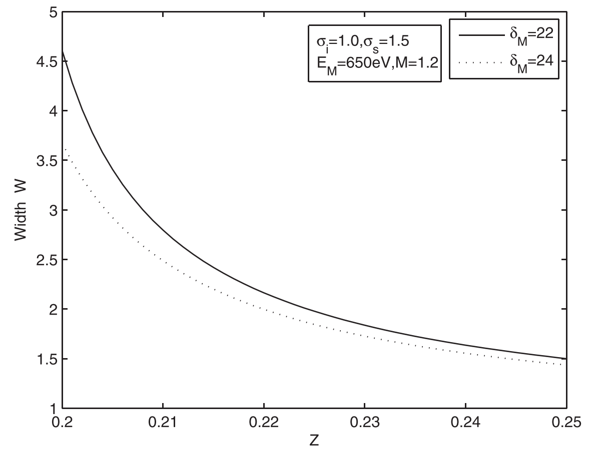

FIG. 3. Plot of the width w of the Dust Acoustic Soliton versus z for different δ_M in case of adiabatic dust charge variation.

$\delta_{\rm M} = 22$ and 24 for the case of adiabatic dust charge variation. Consequent soliton profiles have been plotted in Fig. 4. These three figures show that in the presence of positively charged dust grains, secondary electron emission generates compressive dust acoustic soliton whose amplitude increases and width decreases with increasing secondary electron yield $\delta_{\rm M}$. This is in contrast to the case when equilibrium dust charge is negative. Secondary electron emission with negative equilibrium dust charge generates rarefied dust acoustic soliton whose amplitude decreases and width increases with increasing secondary electron emission.[28] Thus for positive equilibrium dust charge, increasing secondary electron emission increases soliton velocity, whereas it is reduced for negative equilibrium dust charge.

Figures 5 and 6 have been plotted for the coefficient of dissipation μ versus z, and Figs. 7 and 8 have been plotted for the dissipation-dispersion ratio μ/b versus z with $\delta_{\rm M} =$ 22 and 24 at $\nu = 0.5$ (weak nonadiabaticity) and $\nu = 5.0$ (strong nonadiabaticity), respectively. These figures show that dissipation-dispersion ratio μ/b is less than 1 for weak nonadiabaticity ($\nu = 0.5$) and greater than 1 for strong nonadiabaticity ($\nu = 5.0$). This implies for weak nonadiabaticity dust acoustic shock wave is oscillatory, whereas for strong nonadiabaticity it is monotonic . These are confirmed from Figs. 9 and 10, respectively. Moreover, coefficient of dissipation μ and the magnitude of the dissipation-dispersion ratio μ/b at both $\nu = 0.5$ (weak nonadiabaticity) and $\nu = 5.0$ (strong nonadiabaticity) decrease with increasing secondary electron emission. Thus, increasing secondary electron emission in this case reduces monotonicity and gains dispersive character of dust acoustic shock wave. This is opposite to the Ref. 28 where increasing secondary electron emission increased monotonicity of dust acoustic shock wave for equilibrium dust charge negative.

Figures 11 and 12 have been plotted for $\mu^2/4b$ versus z for $\delta_{\rm M} = 22, 24$ at $\nu = 0.5$ and $\nu = 5$, respectively. These two figures show that magnitude of $\mu^2/4b$ is lower for higher secondary electron emission. This enhances the chance of satisfying the cut-off condition $\frac{\mu^2}{4b} < V$ in the permissible range of z which enhances the chance of the nontrivial equilibrium point being a stable focus. This pronounces oscillatory nature of the dust acoustic shock wave which is just opposite to the situation of Ref. 28.

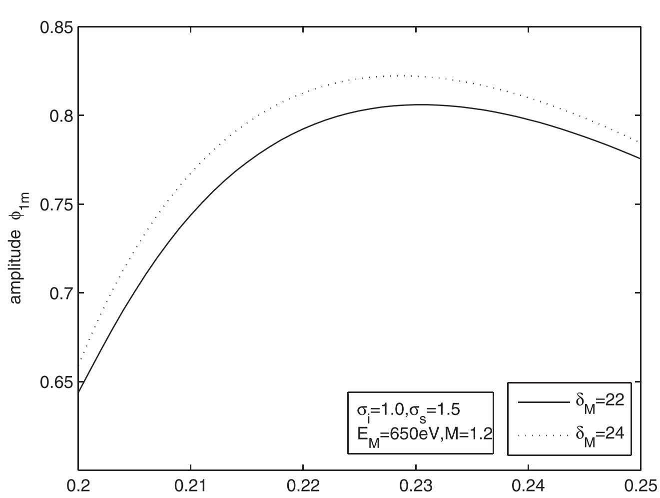

FIG. 2. Plot of the amplitude ϕ_{1m} of the Dust Acoustic Soliton versus z for different δ_M in case of adiabatic dust charge variation.

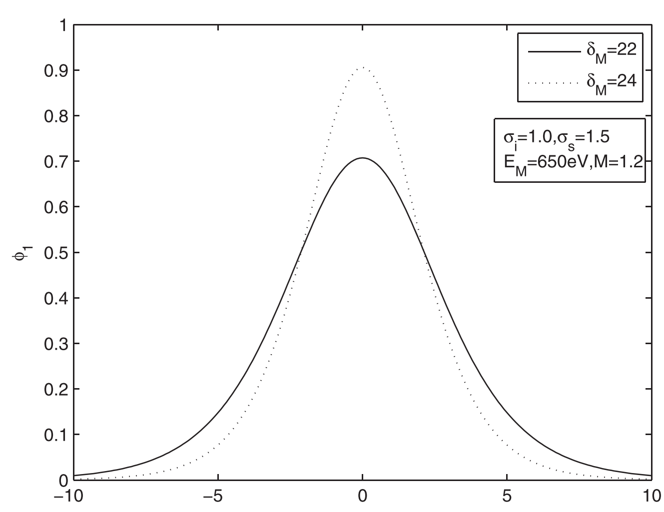

FIG. 4. Plot of the compressive Dust Acoustic Soliton for different δ_M in case of adiabatic dust charge variation.

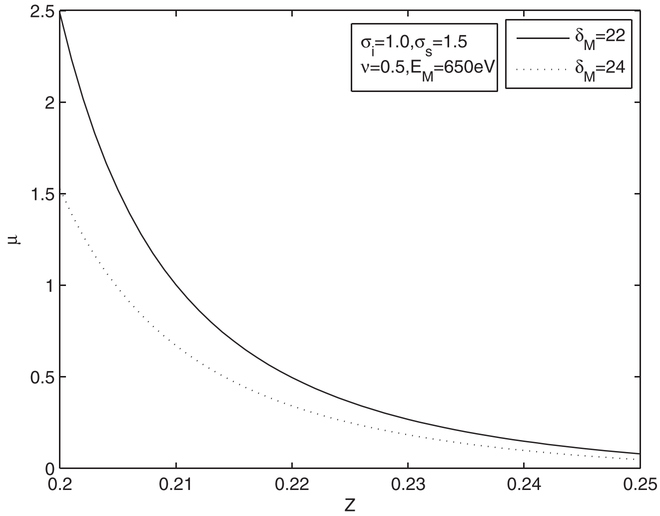

FIG. 5. Plot of the coefficient of the Burgers term μ versus z for different δ_M at $\nu = 0.5$ in case of nonadiabatic dust charge variation.

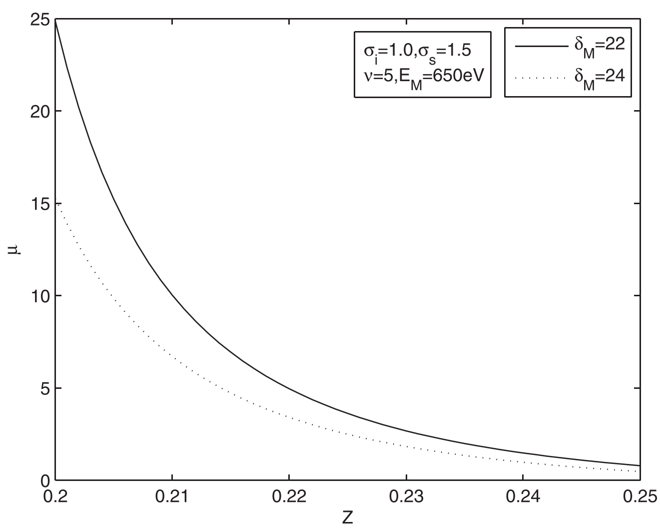

FIG. 6. Plot of the coefficient of the Burgers term μ versus z for different δ_M at $\nu = 5.0$ in case of nonadiabatic dust charge variation.

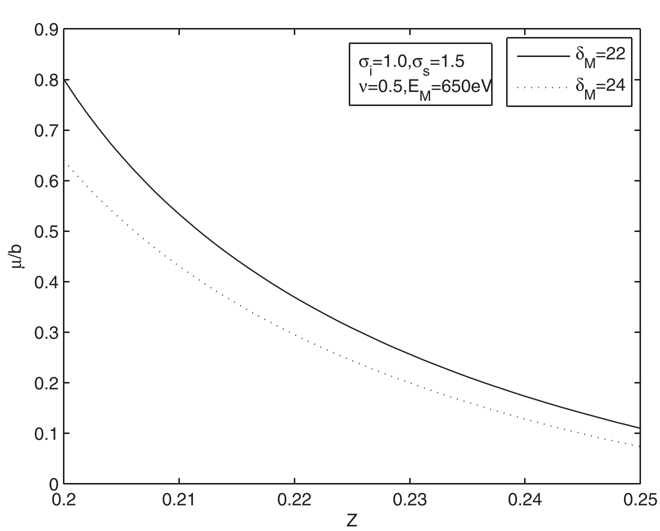

FIG. 7. Plot of the ratio μ/b versus z for different δ_M at $\nu = 0.5$ in case of nonadiabatic dust charge variation.

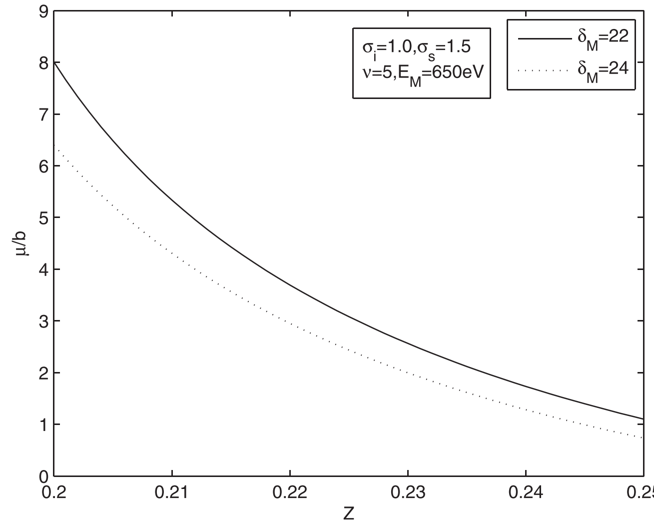

FIG. 8. Plot of the coefficient of the Burger term μ/b versus z for different δ_M when $\nu = 5.0$.

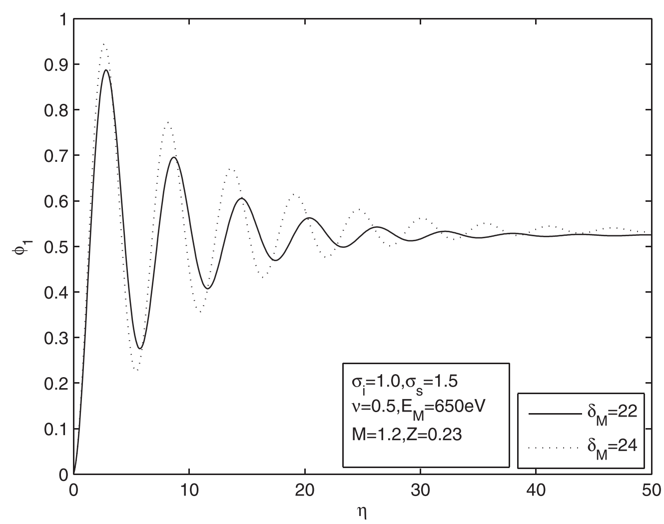

FIG. 9. Oscillatory shock wave for different values of δ_M at $\nu = 0.5$ in case of nonadiabatic dust charge variation.

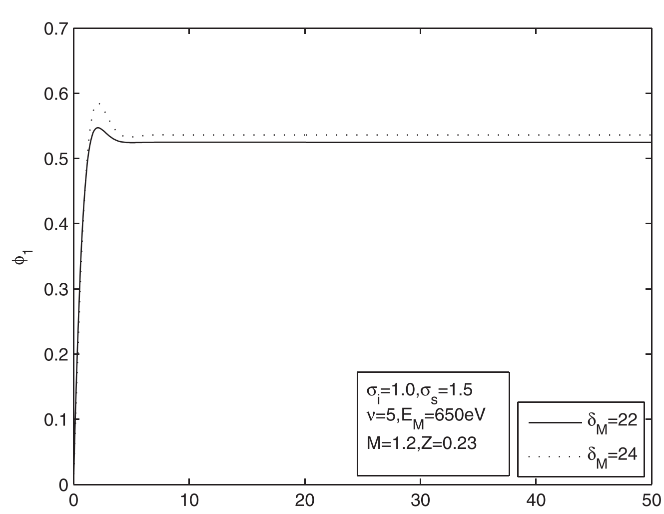

FIG. 10. Monotonic shock wave for different values of δ_M at $\nu = 5$ in case of nonadiabatic dust charge variation.

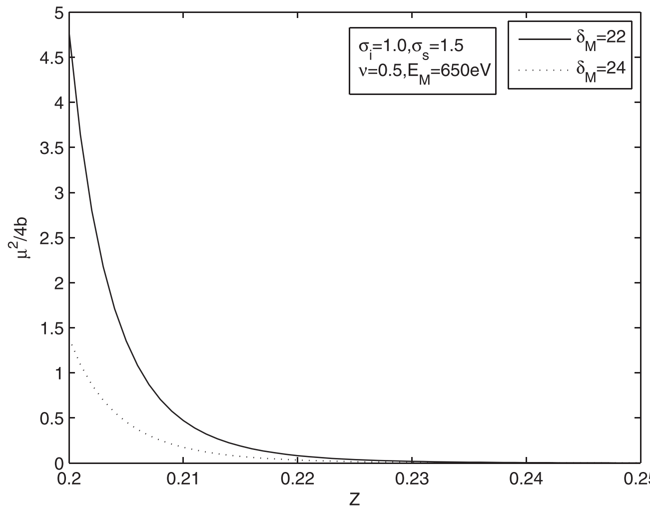

FIG. 11. Plot of the cut off $\mu^2/4b$ versus z for different δ_M at $\nu = 0.5$ in case of nonadiabatic dust charge variation.

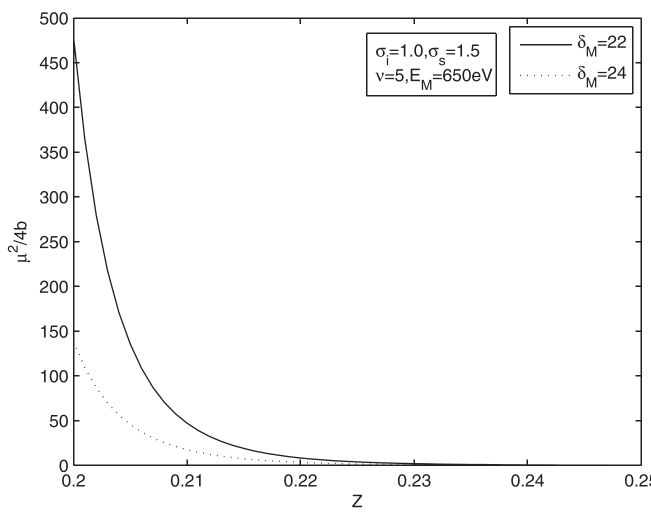

FIG. 12. Plot of the cut off $\mu^2/4b$ versus z for different δ_M at $\nu = 5.0$ in case of nonadiabatic dust charge variation.

V. CONCLUSION

In this paper, we have studied nonlinear propagation of dust acoustic waves in a complex plasma in the presence of secondary electron emission with positive equilibrium dust charge. Both adiabatic and nonadiabatic dust charge variations have been considered. For adiabatic dust charge variation, dust acoustic wave is compressive soliton whose amplitude increases and width decreases with an increase in the strength of the secondary electron emission. For nonadiabatic dust charge variation, oscillatory dust acoustic shock wave propagates at weak nonadiabaticity and monotonic dust acoustic shock wave propagates at strong nonadiabaticity. Stronger secondary electron emission in this case increases the amplitude of both oscillatory and monotonic dust acoustic shock waves and helps to persist oscillation for longer duration. In both cases of adiabatic and nonadiabatic dust charge variations, secondary electron emission favours nonlinear dust acoustic wave propagation when equilibrium dust charge is positive. It is opposite to the case of negative equilibrium dust charge where secondary electron emission does not favour nonlinear dust acoustic wave propagation in case of both adiabatic and nonadiabatic dust charge variations.[28]

[1]L. Austin and H. Starke, Ann. Phys. - Berlin **314**, 271–292 (1902).
[2]H. Bruining, *Physics and Applications of Secondary Electron Emission*, edited by D. W. Fry (Pergamon Press Ltd., Maxwell House, 1954), ISBN: 0080090141.
[3]C. K. Goertz, Rev. Geophys. **27**, 271–292, doi:10.1029/RG027i002p00271 (1989).
[4]B. Walch, M. Horányi, and S. Robertson, Phys. Rev. Lett. **75**, 838 (1995).
[5]M. M. Abbas, D. Tankosic, A. C. LeClair, and J. F. Spann, Astrophys. J. **756**, 41 (2012).
[6]I. Katz, M. Mandell, G. Jongeward, and M. S. Gussenhoven, J. Geophys. Res.-Space **91**, 13739–13744, doi:10.1029/JA091iA12p13739 (1986).
[7]N. Balcon, D. Payan, M. Belhaj, T. Tondu, and V. Inguimbert, IEEE Trans. Plasma Sci. **40**, 282–290 (2012).
[8]M. Rees, A. Stewart, and J. Walker, Space Sci. **17**, 1997–2008 (1969).
[9]C. Baumann, M. Rapp, and A. Kero, Ann. Geophys. **34**, 573–580 (2016).
[10]N. Meyer-Vernet, Astron. Astrophys. **105**, 98 (1982).
[11]E. C Whipple, Rep. Prog. Phys. **44**, 1197 (1981).
[12]M. Horanyi, Ann. Rev. Astrophys. **34**, 383 (1996).
[13]V. W. Chow, D. A. Mendis, and M. Rosenberg, IEEE Trans. Space Sci. **22**(2), 179–186 (1994).
[14]Z. Nemeck, J. Pavlu, J. Safrankova, I. Richterova, and I. Cermack, *Dusty Plasmas in New Millennium* (AIP, NY, 2002), pp. 378–381.
[15]J. Pavlu, J. Safrankova, Z. Nemeck, and A. Velyhan, *Dusty Plasmas in New Millennium* (AIP, NY, 2002), pp. 382–385.
[16]P. Zilavy, Z. Sternovsky, I. Cermak, Z. Nemeck, and J. Safrankova, Vacuum **50**(2), 139–142 (1998).
[17]M. R. Gupta, S. Sarkar, B. Roy, A. Karmakar, and M. Khan, Phys Plasmas **11**, 1850 (2004).
[18]M. R. Gupta, S. Sarkar, B. Roy, A. Karmakar, and M. Khan, Phys. Scr. **71**, 298 (2005).
[19]B. Roy, S. Sarkar, M. Khan, and M. R. Gupta, Phys Lett. A **364**, 291–296 (2007).
[20]S. Sarkar and S. Bhakta, J. Mod. Phys. **7**, 74–86 (2016).
[21]S. Sarkar, B. Roy, S. Maity, M. Khan, and M. R. Gupta, Phys Plasmas **14**, 042106 (2007).
[22]S. Sarkar, S. Maity, B. Roy, and M. Khan, Phys. Scr. **81**, 025504 (2010).
[23]S. Sarkar, S. Maity, and S. Banerjee, Phys. Scr. **84**, 045501 (2011).
[24]S. Ghosh, S. Sarkar, M. Khan, K. Avinash, and M. R. Gupta, Phys Plasmas **10**, 977–983 (2003).
[25]M. R. Gupta, S. Sarkar, S. Ghosh, M. Debnath, and M. Khan, Phys. Rev. E **63**, 046406 (2001).
[26]S. Ghosh, S. Sarkar, M. Khan, and M. R. Gupta, IEEE Trans. Plasma Sci. **29**, 409–416 (2001).
[27]M. M. Abbas, D. Tankosic, J. F. Spann, A. LeClair, M. J. Dube, and J. A. Gaskin, *NLSI Lunar Science Conference* (2008).
[28]S. Bhakta, U. Ghosh, and S. Sarkar, Phys. Plasmas **24**, 023704 (2017).
[29]D. Wen-Shan, Chin. Phys. **13**, 598 (2004).
[30]B. Xie, K. He, and Z. Huang, Phys. Lett. A **247**(6), 403–409 (1998).
[31]S. A. Elwakil, M. A. Zahran, E. K. El-Shewy, and A. E. Mowafy, Adv. Space Res. **48**, 1067–1075 (2011).
[32]J.-H. Chen and N.-X. Wei, Commun. Theor. Phys. **51**(3), 524–528 (2009).
[33]X. Bai-song, H. Kai-fen, and H. Zn-qia, Chin. Phys. Lett. **15**, 12 (1998).
[34]J. Vaverka, I. Richterova, J. Pavlu, J. Sa Frankova, and Z. Nemecek, in *WDs 12 Proceedings of Contributed Papers, Part II* (2012), pp. 152–162.
[35]Y. Wang, C. Guo, X. Jiang, Z. Zhou, and X. Ni, Phys. Plasmas **17**, 113701 (2010).
[36]Y. Wang, X. Guo, Y. Lu, and X. Wang, Phys. Lett. A **380**, 215–221 (2016).
[37]L. Spitzer, Jr., *Physical Process in Interstellar Medium* (John Wiley, NY, 1978).
[38]S. A. Kaplan and S. B. Pikelner, *Interstellar Medium* (Harvard University Press, Cambridge, Mass, 1982).
[39]See www.spacetelescope.org/science/formation_of_stars for Hubble Telescope.